Giant Molecular Clouds in Local Group Galaxies

Leo Blitz
University of California, Berkeley

Yasuo Fukui
Nagoya University

Akiko Kawamura
Nagoya University

Adam Leroy
University of California, Berkeley

Norikazu Mizuno
Nagoya University

Erik Rosolowsky
Harvard-Smithsonian Center for Astrophysics

We present the first comparative study of extragalactic GMCs using complete data sets for entire galaxies and a uniform set of reduction and analysis techniques. We present results based on CO observations for the LMC, SMC, M33, M31, IC10 and the nucleus of M64, and make comparisons with archival Milky Way observations. Our sample includes large spirals and dwarf irregulars with metallicities that vary by an order of magnitude. GMCs in H I rich galaxies are seen to be well-correlated with H I filaments that pervade the galactic disks, suggesting that they form from pre-existing H I structures. Virial estimates of the ratio of CO line strength to H_2 column density, X_{CO}, suggests that a value of 4×10^{20} cm^{-2}(K km s^{-1})$^{-1}$ is a good value to use in most galaxies (except the SMC) if the GMCs are virialized. However, if the clouds are only marginally self-gravitating, as appears to be the case judging from their appearance, half the virial value may be more appropriate. There is no clear trend of X_{CO} with metallicity. The clouds within a galaxy are shown to have the about the same H_2 surface density and differences between galaxies seem to be no more than a factor of ~ 2. We show that hydrostatic pressure appears to be the main factor in determining what fraction of atomic gas is turned into molecules. In the high-pressure regions often found in galactic centers, the observed properties of GMCs appear to be different from those in the found in the Local Group. From the association of tracers of star formation with GMCs in the LMC, we find that about 1/4 of the GMCs exhibit no evidence of star formation and we estimate that the lifetime of a typical GMC in these galaxies is 20–30 Myr.

1. INTRODUCTION

Although a great deal of progress has been made on the topic of star and planet formation since the last Protostars and Planets conference in Santa Barbara, little work has been done to connect what we know about star formation in the Milky Way to star formation in the Universe as a whole. Fundamental limitations include only a weak understanding of how the massive stars form, how clusters and associations form, and the constancy of the IMF. After all, in external galaxies, we generally observe only the effects of massive star formation and the formation of star clusters. Furthermore, knowledge of the initial conditions for star formation at all masses remains elusive both within and outside of the Milky Way.

Since nearly all stars form in Giant Molecular Clouds (GMCs), one way to make progress is to examine the properties of GMCs in a number of different extragalactic environments to see how they differ. From the similarities and differences, it might be possible to make some general conclusions about how star formation varies throughout the Universe. Although individual, extragalactic GMCs had been observed previously at high enough resolution to at least marginally resolve them (e.g., *Vogel et al.*, 1987; *Lada et al.*, 1988), the first attempts to do this in a systematic way were by Christine Wilson (*Wilson and Scoville*, 1990; *Wilson and Reid*, 1991; *Wilson and Rudolph*, 1993;

TABLE 1

LOCAL GROUP GMC DATA

Galaxy	Telescope	Metallicity	Spatial Resolution	Reference
LMC	NANTEN	$0.33\,Z_\odot$	40 pc	1
SMC	NANTEN	$0.1\,Z_\odot$	48 pc	2
IC10	OVRO/BIMA	$0.25\,Z_\odot$	$14 - 20$ pc	3
M33	BIMA	$0.1 - 1.0\,Z_\odot$	$20 - 30$ pc	4
M31	BIMA	$0.5\,Z_\odot$	$26 - 36$ pc	5

References. — (1) *Fukui et al.* (2006) (2) *Mizuno et al.* (2006) (3) *Leroy et al.* (2006) (4) *Engargiola et al.* (2003) (5) *Rosolowsky* (2006)

Wilson, 1994) using the OVRO and BIMA interferometers. Her efforts were hampered by small survey areas in a few galaxies, so general conclusions could only be made by extrapolation. Numerous other authors subsequently studied one or a few extragalactic GMCs, both in the Local Group and beyond. An exhaustive list of their efforts is beyond the scope of the present article.

The situation has changed in the last five years as a result of the construction of the NANTEN telescope in the Southern Hemisphere and the completion of the 10-element BIMA Array. The former made it possible to map the Magellanic Clouds completely with high enough spatial resolution and signal-to-noise to identify all of the GMCs with masses $> 3 \times 10^4 \ M_\odot$; the completion of the BIMA interferometer made it possible to identify GMCs in other, more distant galaxies in the Local Group. Because of their relatively large fields of view, these two telescopes could completely survey nearby galaxies. Thus, the first complete survey of GMCs in *any* galaxy was of the LMC (*Fukui et al.*, 1999; *Mizuno et al.*, 2001b) and not the Milky Way (MW). Although the molecular gas in the MW has been essentially completely mapped, velocity crowding in many directions makes it impossible to generate a full catalog of GMCs. Similarly, the first complete CO surveys of the Magellanic Clouds were by *Cohen et al.* (1988) and *Rubio et al.* (1991), but the resolution was too poor to determine the properties of individual molecular clouds.

In this paper, we review the recent surveys of CO in Local Group galaxies that (1) have sufficient resolution to study individual molecular clouds and (2) span all or most of the target galaxy. We compare the results of observations of GMCs in the four external Local Group galaxies that have been mapped in their entirety in CO: the Large Magellanic Cloud (LMC, *Fukui et al.*, 2001; *Fukui et al.*, 2006), the Small Magellanic Cloud (SMC, *Miznuo et al.*, 2001a; *Mizuno et al.*, 2006), IC 10 (*Leroy et al.*, 2006), and M33 (*Engargiola et al.*, 2003). We have also made observations in a small strip in M31 (*Rosolowsky*, 2006), and we compare the properties of the GMCs in all of these galaxies to clouds in the outer MW (from *Dame et al.*, 2001) us-

ing a uniform set of analytic techniques. The LMC and SMC observations were made with the single-dish NANTEN telescope in Chile, the remaining galaxies were observed with the BIMA millimeter-wave interferometer at Hat Creek, California (combined with obsevations from the Caltech OVRO millimeter interferometer for IC 10). A tabulation of the galaxies we observed, their metallicities and the resolution used to observe them is given in Table 1.

2. THE GALAXIES

In this section, we examine the distribution of CO emission in the surveyed galaxies and we compare the CO to emission in other wavebands.

2.1. The LMC

Fig. 1 shows the molecular clouds detected with the NANTEN Survey (*Fukui et al.*, 2001; *Fukui et al.*, 2006) on an optical image of the LMC. Except for a region near the eastern edge of the galaxy (left side of Fig. 1) below 30 Doradus, the clouds appear to be spatially well-separated and it is possible to pick them out individually by eye. The long string of bright CO emission along the eastern edge of the galaxy is likely composed of several clouds that cannot be separated at this resolution. Some have speculated that this feature is due to hydrodynamical collision between the LMC and SMC (*Fujimoto and Noguchi*, 1990) or ram pressure pileup of gas due to the motion of the LMC through a halo of hot, diffuse gas (*de Boer et al.*, 1998; *Kim et al.*, 1998). Supershells may also be playing a role in the formation of GMCs as in the case LMC4 (*Yamaguchi et al.*, 2001a). A comprehensive comparison between supergiant shells and GMCs shows that only about 1/3 of the GMCs are located towards supershells, suggesting the effects of supershells are not predominant (*Yamaguchi et al.*, 2001b). There is neither an excess nor a deficit of CO associated with the stellar bar, but the bright H II regions are all clearly associated with molecular clouds. Individual clouds are frequently associated with young clusters of

stars. Not every cluster of young stars is associated with a cloud nor does every cloud show evidence of massive star formation. Using this association and the ages of the stellar clusters, we can establish the evolutionary time scale for GMCs (Section 6).
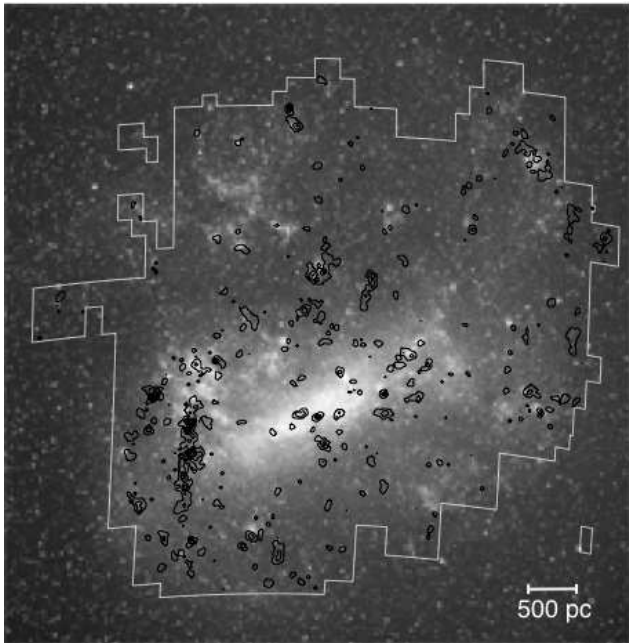

Fig. 1.— Optical image of the LMC with GMCs mapped with the NANTEN telescope indicated within the boundary of the survey area. The CO is well correlated with H II regions. The GMCs are easily identified by eye except for the region south of 30 Doradus where they appear as a vertical line of clouds and the individual GMCs may be overlapping in this region.

2.2. The SMC

Fig. 2 shows the GMCs superimposed on a grayscale image made using the 3.6, 4.5, and 8.0 μm bands from the IRAC instrument on the *Spitzer* Space Telescope (*Bolatto et al.*, 2006). The CO map is from the NANTEN telescope (*Mizuno et al.*, 2006). As in the LMC, the GMCs in the SMC are easily identified by eye. Unlike the LMC, they are not spread throughout the galaxy but appear preferentially on the northern and southern ends of the galaxy. Another grouping is located to the east (left) of the SMC along the H I bridge that connects the LMC and SMC, apparently outside the stellar confines of the galaxy. The *Spitzer* image traces the stellar continuum as well as warm dust and PAH emission. The 8.0 μm emission is associated with the molecular gas traced by CO, but appears to be more extended than the CO emission. The SMC has the lowest metallicity in our sample and provides an opportunity to explore the behavior of molecular gas in chemically primitive environments.

2.3. M33

Fig. 3 shows the locations of GMCs in M33 from the BIMA telescope (*Engargiola et al.*, 2003) superimposed on an Hα image of the galaxy (*Massey et al.*, 2001). The two low-contrast spiral arms (*Regan and Vogel*, 1994) are well-traced by GMCs, but the GMCs are not confined to these arms as is evident in the center of the galaxy. There is good spatial correlation between the GMCs and the H II regions. Once again, the correlation is not perfect and there are GMCs without H II regions and vice versa. Unlike the other images, we show the locations of the GMCs as circles with areas proportional to the CO luminosity of each GMC; the CO luminosity is expected to be proportional to the H$_2$ mass of each GMC. Note that the most massive GMCs ($\sim 10^6$ $M_\odot$) are not found toward the center of the galaxy but along spiral arms north of the galactic nucleus. These massive clouds are relatively devoid of Hα emission. The completeness limit of this survey is about 1.5×10^5 $M_\odot$; thus there are presumably many lower mass clouds below the limit of sensitivity. Many of these low mass clouds are likely associated with the unaccompanied H II regions in the figure.

2.4. IC 10

Fig. 4 is an image of the GMCs in IC 10 from a 50 field CO mosaic with the BIMA telescope (*Leroy et al.*, 2006) superimposed on a 2 μm image of the galaxy made from 2MASS data (*Jarrett et al.*, 2003). As with the Magellanic Clouds and M33, the GMCs show no obvious spatial correlation with old stellar population – some massive clouds are found where there are relatively few stars.
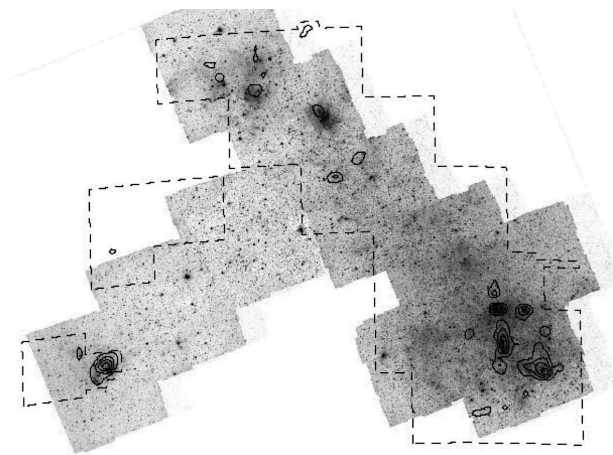

Fig. 2.— GMCs in the SMC observed with the NANTEN telescope overlayed on an a near-infrared image of the galaxy from the *Spitzer* Space Telescope (*Bolatto et al.*, 2006). The lines indicate the survey boundary. The CO clouds are clearly associated with regions of transiently heated small grains or PAHs that appear as dark, nebulous regions in the image.
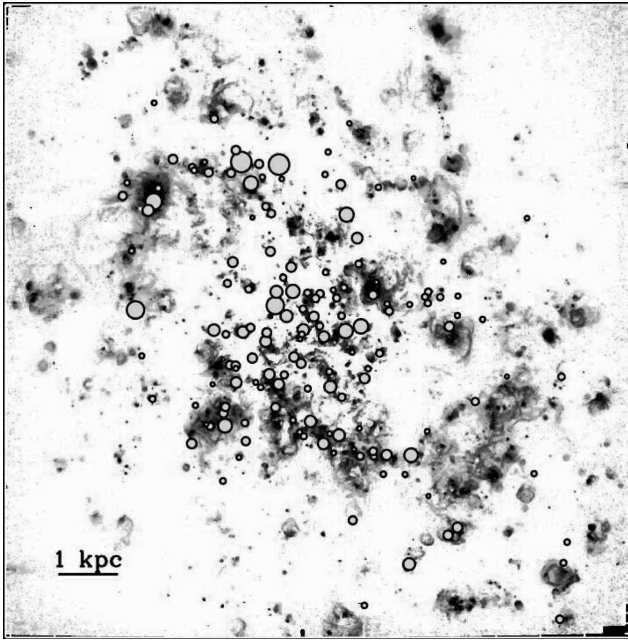
Fig. 3.— The locations of GMCs in M33 as derived from the 759 field BIMA mosaic of *Engargiola et al.* (2003). Since sources of CO emission in a map would be too small to identify in the figure, the locations of GMCs are instead indicated by light gray circles. The area of the circles is scaled to the CO luminosity which should be proportional to the H_2 mass. The GMC locations are overlayed on a continuum subtracted Hα image of the galaxy (*Massey et al.*, 2001). There is significant correlation between the GMCs and massive star formation as traced by Hα.

Fig. 4.— The GMCs in IC 10 made from a 50 field mosaic of the galaxy with the BIMA telescope overlayed on a 2 μm image of the galaxy from the 2MASS survey. The dark gray area corresponds to CO brightness above 1 K km s^{-1}; the light gray area corresponds to CO brightness above 10 K km s^{-1}. The black region in the center has the highest stellar surface density. The rms noise of the CO data is ~ 0.3 K km s^{-1} in each channel map; the peak value in the integrated intensity map is 48 K km s^{-1} (*Leroy et al.*, 2006).

2.5. The Correlation with H I

The distribution of GMCs in these four galaxies shows little correlation with old stars (see Figs. 1 and 4). The obvious correlations with Hα (Figs. 1 and 3) and young stellar clusters (Fig. 1) are expected since these trace the star formation that occurs within GMCs. That the correlation is not perfect can be used to deduce information about the evolution of the clouds (Section 6). To examine the relationship of GMCs to the remainder of the neutral ISM, we plot the locations of CO emission on top of H I maps of these four galaxies in Fig. 5. A strong correlation between the atomic and molecular gas is immediately apparent. Every GMC in each of the galaxies is found on a bright filament or clump of H I, but the reverse is not true: there are many bright filaments of H I without molecular gas. In M33, the largest of the fully mapped galaxies, the ratio of H I to CO in the filaments in the center of the galaxy is smaller than in the outer parts. In the LMC, the CO is generally found at peaks of the H I, but most of the short filaments have no associated CO. In the SMC, the H I is so widespread that the CO clouds appear as small, isolated clouds in a vast sea of H I. Apparently, H I is a necessary but not a sufficient condition for the formation of GMCs in these galaxies.

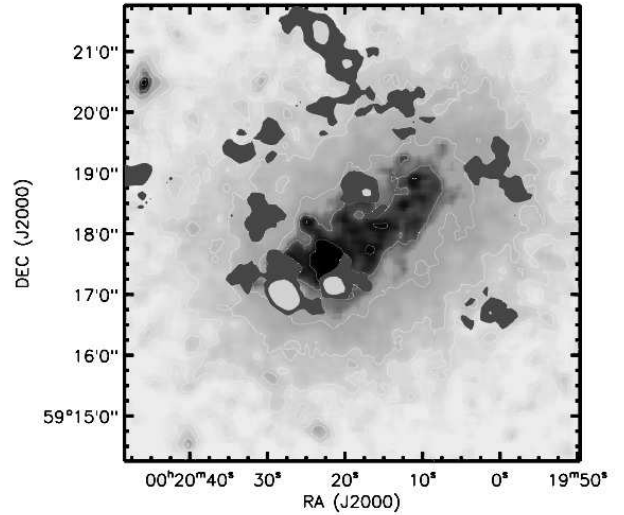Figs. 1 – 4 show that the molecular gas forms from the H I, rather than the H I being a dissociation product of the molecular clouds as some have advocated (e.g., *Allen*, 2001). First, in all four galaxies the H I is much more widespread than the detected CO emission. Thus, most of the H I cannot be dissociated H_2 without violating mass conservation if the GMC lifetimes are as short as we derive in Section 6. Second, there is no CO associated with most of the filaments in the LMC, M33, and IC 10 and the column density of these CO-free filaments is about the same as the column density of filaments which have CO emission. Because there is no transition in H I properties at radii where one observes CO, and the radii where it is absent, it is difficult to imagine that two separate origins for the H I would produce a seamless transition. Finally, the H I in the filaments between GMCs has the wrong geometry to be a dissociation product; there is too much gas strung out along the filaments to have come from dissociation of the molecular gas.

2.6. Implications for GMC Formation

What can the morphology of the atomic gas tell us about GMCs and their formation? All the H I images are characterized by filamentary structures that demarcate holes in the atomic distribution. In IC 10, there is good evidence that some of the holes are evacuated by the action of supernovae or stellar winds which sweep up the atomic gas

4

into the observed filamentary structure (*Wilcots and Miller*, 1998). In contrast, most of the large holes observed in the M33 H I distribution are *not* likely to be caused by supernovae. The large holes require about 10^{53} ergs to evacuate, but there are no obvious stellar clusters remaining at the center of the holes. Furthermore, x-ray emission is not concentrated in the holes. The large holes in M33 are thus likely to have a gravitational or density-wave origin. Small holes with $D < 200$ pc, on the other hand, are found to be well correlated with OB associations (*Deul and van der Hulst*, 1987); these tend to be concentrated toward the center of the galaxy.

This leads to some qualitative conclusions about the formation of GMCs and ultimately the star formation that occurs within them. Because the CO forms from H I filaments and not the other way around, it is the filaments in a galaxy that must form first as precursors to the GMCs. In some of the galaxies, such as M33 and apparently in the LMC and the SMC, most of the filaments are not associated with energetic phenomena. This clearly rules out the self-propagating star formation picture that was promoted some years back by *Gerola and Seiden* (1978) for most of our galaxies. In their picture, GMC formation and thus star formation propagates by means of supernovae that explode in regions of a galaxy adjacent to a previous episode of star formation. However, in IC 10, because there is evidence that some of the H I morphology may be the result of energetic events from previous generations of stars, self-propagating star formation may be a viable mechanism. *The critical element of GMC formation across all these systems appears to be the assembly of H I filaments, though the mechanism that collects the atomic gas appears to vary across the systems.*

But why, then, do some filaments form GMCs and not others? We argue in Section 5, that it is the result of the pressure to which filaments are subjected.

3. MOLECULAR CLOUD PROPERTIES

Our main goal in this section is to compare the properties of GMCs made with different telescopes, resolutions, and sensitivities. We use GMC catalogs from the studies of the four galaxies listed above, and we supplement our work with a sample of GMCs in M31 (*Rosolowsky*, 2006) as well as a compilation of molecular clouds in the outer Milky Way as observed by *Dame et al.* (2001) and cataloged in *Rosolowsky and Leroy* (2006).

To aid in the systematic comparison of cloud properties, *Rosolowsky and Leroy* (2006, hereafter RL06) have recently published a method for minimizing the biases that plague such comparisons. For example, measurement of the cloud radius depends on the sensitivity of the measurements, and RL06 suggest a robust method to extrapolate to the expected radius in the limit of infinite sensitivity. They also suggest a method to correct cloud sizes for beam convolution, which

has been ignored in many previous studies of extragalactic clouds. We use the RL06 extrapolated moment method on all of the data used in this paper since it is least affected by relatively poor signal-to-noise and resolution effects. We have also applied the RL06 methodology to the outer Milky Way data of *Dame et al.* (2001) rather than relying on published properties (e.g., *Heyer et al.*, 2001). It is for this reason that we have not included the cloud properties of *Solomon et al.* (1987) in our plots, but we do make comparisons to their work at the end of this section. Except where noted, we consider only clouds that are well-resolved by the telescope beam; the GMCs must have angular diameters at least twice that of the beam used to observe them.

Are we seeing single or multiple objects in the beam? The issue of velocity blending of multiple clouds in the beam is much less of an issue in extragalactic observations than in the Galactic case, where the overwhelming majority of GMCs are observed only in the Galactic plane. Extragalactic observations of all but the most highly inclined galaxies do not suffer from this problem and as can be seen in Figs. 1 – 4, the clouds are, in general, spatially well separated, ensuring that we are almost always seeing only a single GMC along the line of sight.

One of the long debated questions related to GMCs is: how does metallicity affect the value of X_{CO}, the conversion factor from CO line strength to H_2 column density? Fig. 6 is a plot of the virial mass of the GMCs as a function of CO luminosity. Diagonal lines are lines of constant X_{CO}. A compilation of X_{CO} values is given in Table 2. We note first that most of the points lie above the dashed line that indicates the value determined from gamma-rays in the Milky Way (*Strong and Mattox*, 1996). A value of $X_{\mathrm{CO}} = 4 \times 10^{20}$ cm^{-2}(K km s^{-1})$^{-1}$ would allow virial masses to be derived to within about a factor of two for all of the GMCs in our sample, with the clouds in the SMC and the outer Galaxy requiring a somewhat higher value.

Note, however, that the SMC clouds are systematically higher in this plot than the GMCs for any other galaxy, and that the GMCs in IC 10 are systematically a bit lower. Solving for X_{CO} in the SMC, gives a value of 13.5×10^{20} cm^{-2}(K km s^{-1})$^{-1}$, more than a factor of 3 above the mean. In contrast, IC 10 yields $X_{\mathrm{CO}} = 2 \times 10^{20}$ cm^{-2}(K km s^{-1})$^{-1}$. Surprisingly, the galaxies differ in metallicity from one another only by a factor of two, and both are much less than solar. In M33, the metallicity decreases by almost an order of magnitude from the center out (*Henry and Howard*, 1995), but *Rosolowsky et al.* (2003) find no change in X_{CO} with radius. Although metallicity may be a factor in determining X_{CO} in different galaxies, there is no clear trend with metallicity alone – other factors appear to be as important as the metallicity in determining X_{CO}.

The discrepancy between the Galactic gamma-ray value of 2×10^{20} cm^{-2}(K km s^{-1})$^{-1}$ and the virial value we derive here is not necessarily a problem. Taken at face value, it may be telling us is that the GMCs are not in virial equilibrium, but are nearly gravitationally neutral: the overall
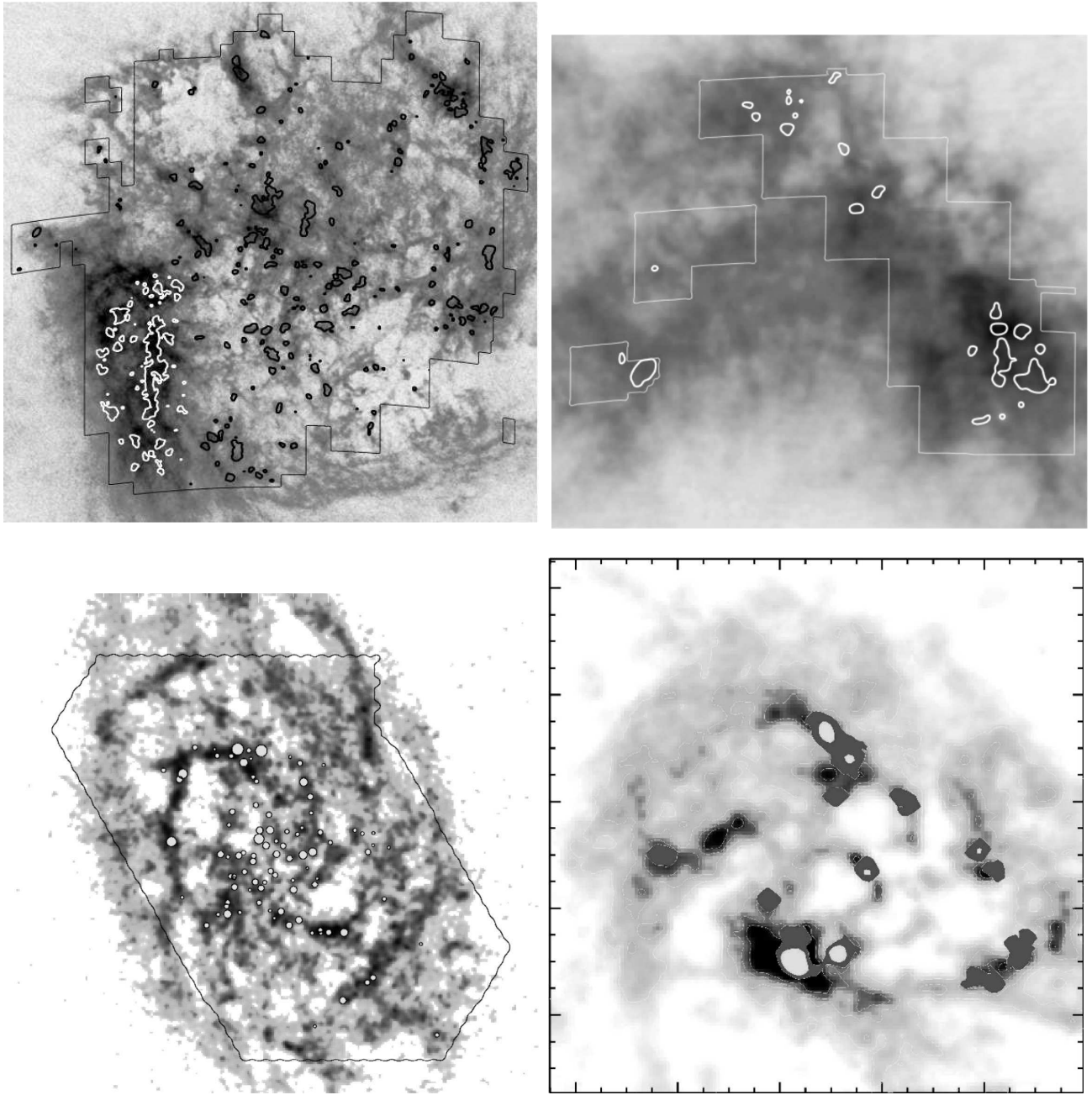
Fig. 5.— CO emission overlayed on maps of H I emission for the LMC (top left), the SMC (top right), M33 (bottom left) and IC 10 (bottom right). The H I maps are the work of *Kim et al.* (2003, LMC), *Stanimirović et al.* (1999, SMC), *Deul and van der Hulst* (1987, M33), and *Wilcots and Miller* (1998, IC10). Contours of the CO emission are shown in each case except for M33 where the emission is indicated as circles with area proportional to the flux. Where appropriate, the boundaries of the surveys are indicated. CO emission is found exclusively on bright filaments of atomic gas though not every bright H I filament has CO emission.
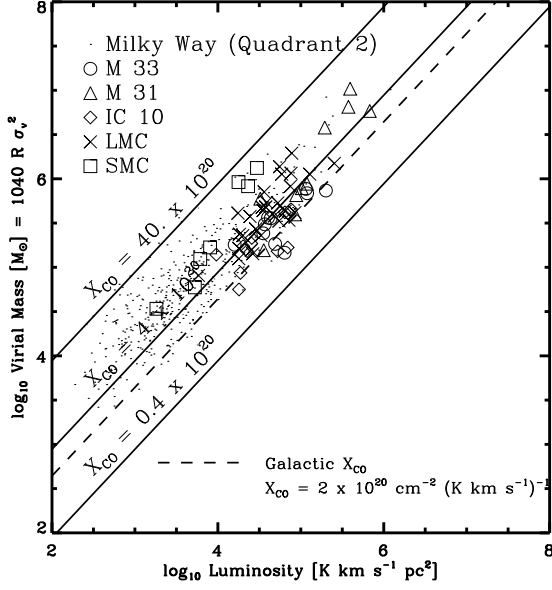
TABLE 2
X_{CO} ACROSS THE LOCAL GROUP

Galaxy	Mean X_{CO} $\times 10^{20}$ cm^{-2} (K km s^{-1})$^{-1}$	Scatter in X_{CO}[a]
LMC	5.4 ± 0.5	1.7
SMC	13.5 ± 2.6	2.2
M33	3.0 ± 0.4	1.5
IC10	2.6 ± 0.5	2.2
M31	5.6 ± 1.1	2.7
Quad 2[b]	6.6 ± 0.6	2.0
Local Group[c]	5.4 ± 0.5	2.0

[a]Scatter is a factor based on median absolute deviation of the log.

[b]Clouds with luminosities corresponding to $M_{Lum} \geq 5 \times 10^4$ M$_\odot$ (for $X_{CO} = 2 \times 10^{20}$)

[c]Excluding Milky Way.

Fig. 6.— Plot of the virial mass of the GMCs in our sample as a function of luminosity. The value of X_{CO} from gamma-ray investigations in the Milky Way (*Strong and Mattox*, 1996) is shown by the dashed line. The plot shows that while there are some differences in X_{CO} from galaxy to galaxy, except for the SMC, a value of $X_{CO} = 4 \times 10^{20}$ cm^{-2}(K km s^{-1})$^{-1}$ can be used for all of the other galaxies to a reasonable degree of approximation.
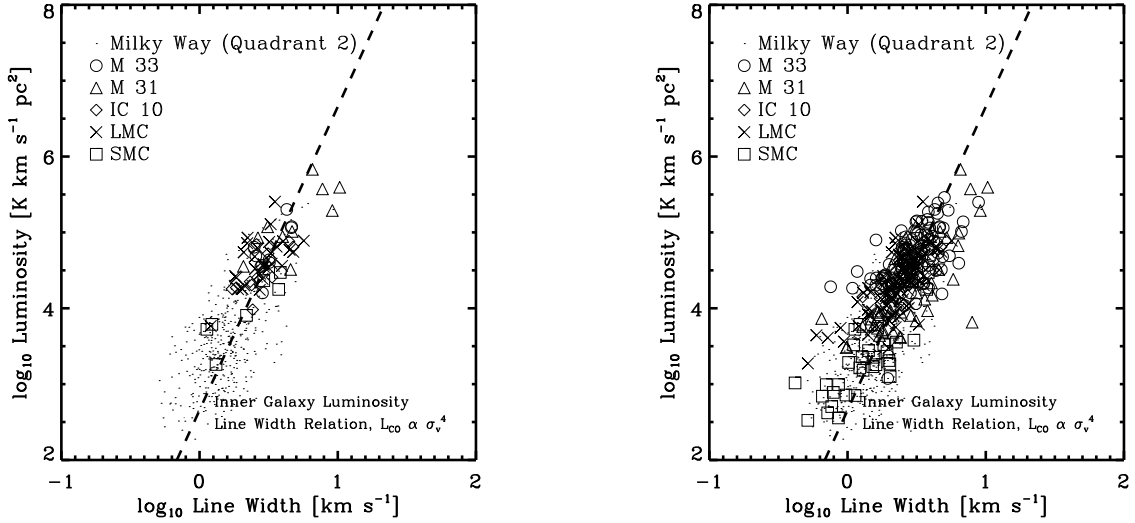

Fig. 7.— *(Left)* Luminosity vs. Line width plot for all of the resolved clouds in our survey. The dashed line, $L_{CO} \propto \sigma_v^4$, with a single constant of proportionality is a good representation of the data. *(Right)* The same as the left-hand panel but including the unresolved clouds in our sample. The dashed line remains a good representation of the data even with much more data included.

7

potential energy is equal to the kinetic energy. The gamma-ray value of X_{CO} is independent of the dynamical state of the cloud, thus, uncertainties about the self-gravity of GMCs do not come into play. Since GMCs do not look as if they are in virial equilibrium (they are highly filamentary structures and do not appear to be strongly centrally concentrated), these two different values of X_{CO} are consistent if the clouds are only marginally self-gravitating.

The left-hand panel of Fig. 7 is a plot of the CO luminosity of GMCs as a function of line width. It may be thought of as a plot of H_2 mass vs. line width for a single, but undetermined, value of X_{CO}. The dashed line, is the relation $L_{CO} \propto \sigma_v^4$, is not a fit, but is a good representation of the data for both the five external galaxies in our sample as well as for the outer Milky Way. The scatter in the relationship is 0.5 dex, or a factor of 3 over three orders of magnitude in luminosity. If the GMCs are self-gravitating, then they obey

$$M = 5R\sigma_v^2/(\alpha G) \qquad (1)$$

where α is a constant of order unity. Provided the CO luminosity is proportional to the mass of a GMC, the plot shows that $M(H_2) \propto \sigma_v^4$; thus

$$\sigma_v \propto R^{0.5} \quad \text{and} \quad M/R^2 = \text{constant}. \qquad (2)$$

These two relations are shown on the left- and right-hand sides of Fig. 8 respectively.

The advantage of a luminosity-line width plot, especially for extragalactic studies is that one need not resolve the individual clouds, since the luminosity, and by implication, the mass, is independent of resolution. One need only be sure that individual GMCs are isolated in the beam. The right-hand panel in Fig. 7 shows all of the individual clouds identified in the galaxy surveys, most of which are unresolved. We see that the clouds populate the same $L_{CO} \propto \sigma_v^4$ line as in the left-hand panel. This plot demonstrates probably better than any other that the GMCs in our sample are much more alike than they are different.

The left-hand side of Fig. 8 is the size-line width relation for the GMCs in our sample. The dashed line is the size-line width relation for GMCs in the inner region of the Milky Way from *Solomon et al.* (1987). First, we note that the correlation for the extragalactic clouds is very weak. However, if we add the outer Galaxy clouds, the correlation does seem to be consistent with a power law relation $\sigma_v \propto R^{0.5}$. However, there is a clear offset from the relation determined for the inner Galaxy (dashed line, *Solomon et al.*, 1987). At least part of this offset can be attributed to differences in the methods used to measure cloud properties. The sense of the offset is that for a given cloud radius, inner Milky Way clouds have larger line widths. This may be partially due to the relatively high value of T_A used by *Solomon et al.* (1987) to define the cloud radius, implying that the clouds might be inferred to be smaller for a given value of σ_v.

But part of the offset may also be real. We see that there is a clear separation of the clouds by galaxy in the plot. The

IC 10 clouds lie to the left of the diagram, while the LMC clouds lie to the right. The SMC clouds tend to lie at the bottom of the group. The apparently weak correlation of extragalactic clouds is probably due to the small dynamic range in the plot compared to the measurement error in the cloud properties; the rms scatter in Fig. 8 (left) is only 0.2 dex, or less than a factor of two. We therefore conclude that the GMCs in our sample are consistent with a power law relation $\sigma_v \propto R^{0.5}$. There are, however, real differences in the coefficient of proportionality, and this gives rise to some of the scatter in the relationship. The size-line width relationship arises from the turbulent nature of the molecular gas motions. Differences in the constant of proportionality imply variations in the normalization of the turbulent motions of GMCs in different galaxies, independent of cloud luminosity.

These conclusions help to explain Fig. 8 (right), which is a plot of luminosity vs. radius. Assuming that luminosity is proportional to mass, at least within a single galaxy, we can plot lines of constant surface brightness. After all, Fig. 6 suggests that the clouds have a constant surface brightness. In fact, it appears that for a given galaxy, the individual GMCs are strung out along lines of constant surface density, but with each galaxy lying on a different line. The SMC clouds, for example, have a mean surface density of $10\ M_{\odot}$ pc^{-2}, but the IC 10 clouds have a mean surface density > $100\ M_{\odot}\ pc^{-2}$. A direct interpretation of Fig. 8 (right) implies that for a given radius, the SMC clouds are less luminous than the rest, and the IC 10 clouds are more luminous. Another way of saying this is that for a given cloud luminosity, the SMC clouds are larger, as are the LMC clouds, only less so. This difference disappears, for the most part, if we consider the mass surface density rather than the surface brightness. In that case one must multiply the luminosity of the GMCs in each galaxy by its appropriate value of X_{CO}. When that is done, the difference in the mean surface density from galaxy to galaxy is less than a factor of two.

In Fig. 7 we see that the GMCs in the SMC are well-separated from the GMCs in M31, implying that the median luminosity of the two sets of clouds is different by nearly two orders of magnitude. The differences due to X_{CO} are only a factor of about 4; but is the distribution of GMC masses in the two systems really different? There are not enough clouds to measure a mass spectrum in the SMC, but Fig. 9 shows the mass distribution of molecular clouds normalized to the survey area for the other five galaxies. Power-law fits to the masses of all cataloged molecular clouds above the completeness limit give the index of the mass distributions listed in Table 3. All of the galaxies have remarkably similar mass distributions except for M33, which is much steeper than the others. In addition, the mass distributions in M31 and the LMC show a truncation at high mass similar to that found in the inner Milky Way (e.g., *Williams and McKee*, 1997) suggesting that there is a characteristic cloud mass in these systems. In addition, *Engargiola et al.* (2003) also argue for a characteristic cloud mass in M33 but it is not at the high mass
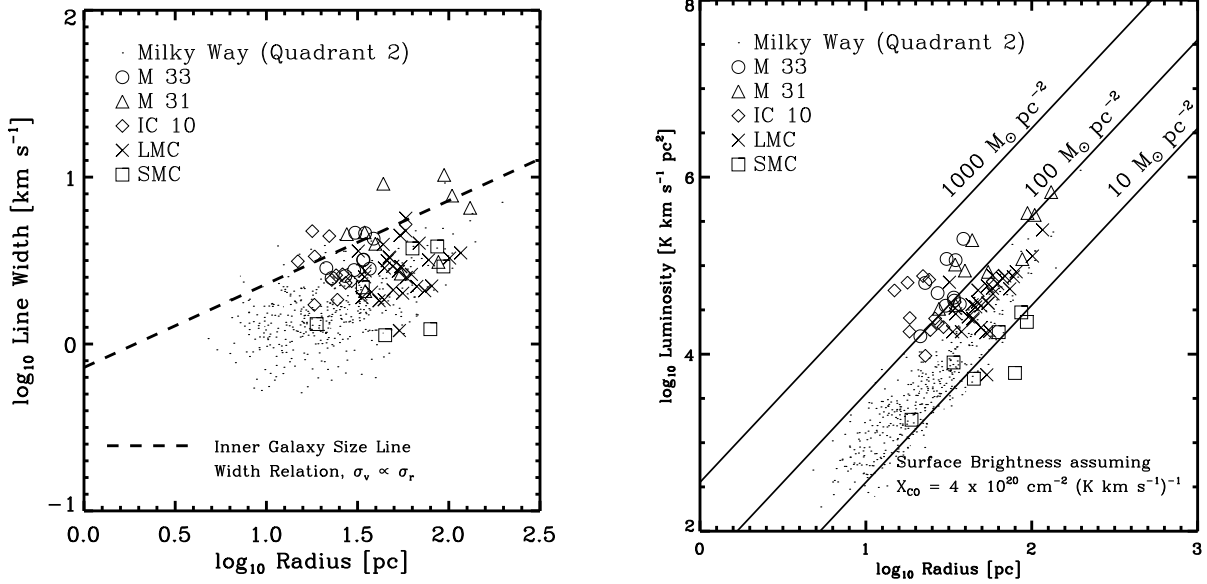
Fig. 8.— *(left)* Line width-size relation for the GMCs in our sample. The dashed line is the relation found for the GMCs in the inner Milky Way, showing a clear offset from the extragalactic GMCs. *(Right)* Luminosity vs. Radius relation for the GMCs in our sample. Solid lines are lines of constant surface density assuming $X_{CO} = 4 \times 10^{20}$ cm^{-2}(K km s^{-1})$^{-1}$. The galaxies show clear differences in CO luminosity for a given cloud radius.

Table 3.   Mass Distributions of the 5 Galaxies
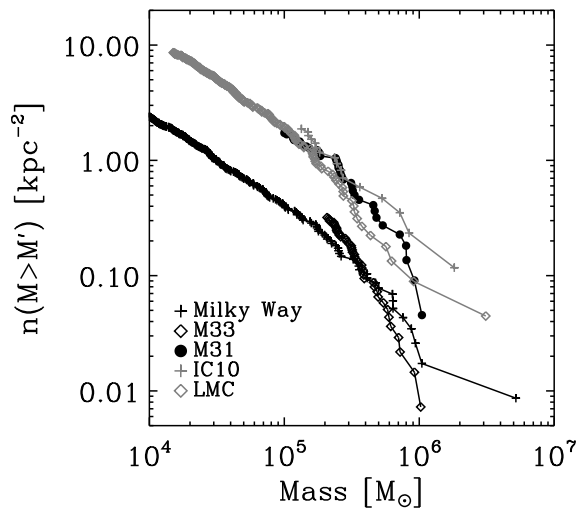
Galaxy	Index
LMC	-1.74 ± 0.08
IC10	-1.74 ± 0.41
M33	-2.49 ± 0.48
M31	-1.55 ± 0.20
Outer MW	-1.71 ± 0.06

Fig. 9.— Cumulative mass distribution for the Galaxies in our sample. The mass distributions have been normalized by the area surveyed in each galaxy. In this figure, we use all clouds above the completeness limits in each survey, whether or not the clouds are resolved. All of the galaxies look similar except for M33 which has a steeper mass spectrum than the others.

9

end, as it is for the LMC and M31; rather it has a value of $4 - 6 \times 10^4$ M$_\odot$. The variation in the mass distributions is unexplained and may offer an avenue to understanding differences in star formation rates between galaxies.

4. THE ROLE OF HYDROSTATIC PRESSURE

A number of authors have speculated on the role that hydrostatic pressure plays in the formation of molecular clouds in the centers of galaxies (*Helfer and Blitz*, 1993; *Spergel and Blitz*, 1992), and galactic disks (*Elmegreen*, 1993; *Wong and Blitz*, 2002; among others). *Blitz and Rosolowsky* (2004) showed that if hydrostatic pressure is the only parameter governing the molecular gas fraction in galaxies, then one predicts that the location where the ratio of molecular to atomic gas is unity occurs at constant *stellar* surface density. They probed this prediction and found that the constancy holds to within 40% for 30 nearby galaxies.

The functional form of the relationship between hydrostatic pressure and molecular gas fraction has recently been investigated by *Blitz and Rosolowsky* (2006) for 14 galaxies covering 3 orders of magnitude in pressure. Hydrostatic pressure is determined by

$$P_{hydro} = 0.84(G\Sigma_*)^{0.5}\Sigma_g \frac{v_g}{(h_*)^{0.5}}. \qquad (3)$$

The quantities v_g, the gas velocity dispersion, and h_*, the stellar scale height, vary by less than a factor of two both within and among galaxies (*van der Kruit and Searle*, 1981a,b; *Kregel et al.*, 2002). The quantities Σ_*, the stellar surface density, and Σ_g, the gas surface density, can be obtained from observations. The results for 14 galaxies is given in Fig. 10.

The figure shows that the galaxies all have similar slopes for the relationship: $\Sigma_{\rm H2}/\Sigma_{\rm HI} \propto P^{0.92}$, very nearly linear. Moreover, except for three galaxies, NGC 3627, NGC 4321, and NGC 4501, all have the same constant of proportionality. The three exceptional galaxies all are interacting with their environments and may be subject to additional pressure forces. It is important to point out that we expect this pressure relation to break down at some lower scale no smaller than the scale of a typical GMC, $\sim$50 pc. However, on the scale of the pressure scale height, typically a few hundred parsecs, the pressure should be more or less constant both vertically and in the plane of a galaxy.

The two axes in Fig. 10 are not completely independent; both are proportional to $\Sigma_{\rm H2}$. However, each axis is also dependent on other quantities such as $\Sigma_{\rm HI}$ and Σ_*. Since Σ_* varies by a larger amount in a given galaxy than Σ_{H_2}, because $\Sigma_{\rm HI}$ dominates at low pressures ($P/k < 10^5$ cm^{-3} K) and because both axes have different dependencies on $\Sigma_{\rm H2}$, the constancy of the slopes and the agreement of the intercepts cannot be driven by the common appearance of $\Sigma_{\rm H2}$ on each axis. A more detailed discussion of this point is given in *Blitz and Rosolowsky* (2006).
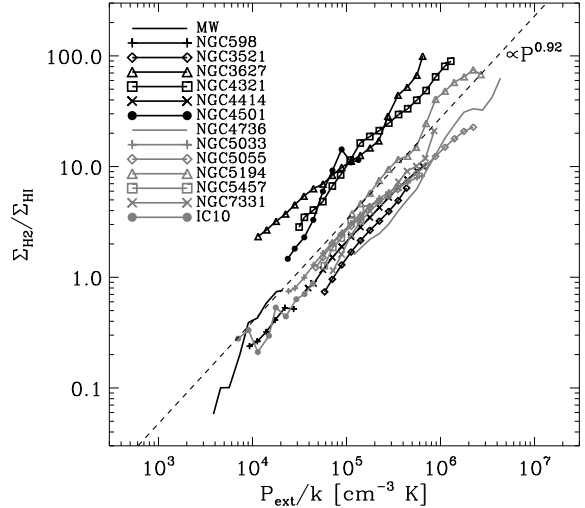

Fig. 10.— Plot of the ratio of molecular to atomic surface density as a function of hydrostatic pressure for 14 galaxies. The plot covers 3 magnitudes in pressure and molecular fraction.

As of this writing we do not know how the LMC and the SMC fit into this picture; no good map giving the stellar surface density for these objects is currently available. Although we do not know the stellar scale heights for these galaxies, because of the weak dependence on h_* in Equation 3, this ignorance should not be much of a difficulty. The results for the SMC are particularly interesting because of its low metallicity and low dust-to-gas ratio (*Koorneef*, 1984; *Stanimirovic et al.*, 2000). Since the extinction in the UV is significantly smaller than in other galaxies, one might expect higher pressures to be necessary to achieve the same fraction of molecular gas in the SMC, though care must be taken since CO may be compromised as a mass tracer in such environments.

The following picture for the formation of molecular clouds in galaxies is, then, suggested by the observations. Density waves or some other process collects the atomic gas into filamentary structures. This process may be the result of energetic events, as is thought to be the case for IC 10, or dynamical processes, as is primarily the case for M33. Depending on how much gas is collected, and where in the gravitational potential of the galaxy the gas is located, a fraction of the atomic hydrogen is turned in molecular gas. In very gas-rich, high pressure regions near galactic centers, this conversion is nearly complete. But some other process, perhaps instabilities, collects the gas into clouds. Whether this is done prior to the formation of GMCs, or after is not clear.

5. GMCS IN STARBURST GALAXIES

In many galaxies the average surface density of molecular gas is much greater than the surface densities of indi-

vidual GMCs shown in Fig. 8 (*right*; *Helfer et al.*, 2003). These regions of high surface density can be as much as a kiloparsec in extent. Indeed, about half of the galaxies in the BIMA SONG survey (*Helfer et al.*, 2003) have central surface densities in excess of 100 $M_\odot$ pc^{-2}. Moreover, regions with high surface densities of molecular gas are invariably associated with dramatically enhanced star formation rates (*Kennicutt*, 1998). In regions of such high surface density, are there even individual, identifiable GMCs? If so, do they obey the same relations shown in Figs. 6 – 8?

Several recent studies have begun to attack these questions. The only such molecule-rich region in the Local Group is in the vicinity of the Galactic Center where cloud properties were analyzed by *Oka et al.* (2001). They found that clouds in the Galactic center were smaller, denser and had larger line widths than the GMCs in the Galactic disk. For targets beyond the Local Group, achieving the requisite spatial resolution to study individual GMCs requires significant effort. To date, only a few extragalactic, molecule-rich regions have been studied. *Keto et al.* (2005) show clouds in M82 to be roughly in virial equilibrium. At the high surface densities of molecular gas observed in M82, this requires clouds to be smaller and denser than those found in the Galactic disk. Similarly, *Rosolowsky and Blitz* (2005) observed the inner region of the Galaxy M64, which has a surface density of ~ 100 $M_\odot$ pc^{-2} over the inner 300 pc of the galaxy. They found 25 GMCs with densities 2.5 times higher, and are 10 times more massive, on average, than typical disk GMCs. This conclusion is quite robust against differences in cloud decomposition because if some of the clouds they identify are in fact blends of smaller clouds, then the derived densities are lower limits, reinforcing their conclusions. In M64, *Rosolowsky and Blitz* (2005) examine many of the relationships shown in Figs. 7 and 8 and find that all are significantly different.

5.1. GMC Formation in Galactic Centers

The peak H_2 surface density in the central 1 kpc of M64 is about 20 times the H I surface density (*Braun et al.*, 1994; *Rosolowsky and Blitz*, 2005), which is typical of many galaxies (*Helfer et al.*, 2003). In such regions, the formation of GMCs cannot take place by first collecting atomic hydrogen into filaments and then turning the gas molecular. If the gas is cycled between the atomic and molecular phases, as is required by the presence of H II regions in the central regions of M64, then continuity requires that the amount of time that the gas remains in each phase is roughly equal to the ratio of surface densities at each particular radius. Thus, gas ionized by the O stars must quickly return to the molecular phase, which is catalyzed by the very large pressures in the central region (Section 4). More than likely, the GMCs are formed and destroyed without substantially leaving the molecular phase, unlike what happens in the disks. Indeed, *Rosolowsky and Blitz* (2005) present evidence for a diffuse molecular component that is not bound into GMCs. Thus it seems likely that, as in galactic disks, the formation of

structure (filaments?) in galactic nuclei occurs before the formation of the GMCs. The gas, though, is largely molecular prior to the formation of the clouds.

Measuring the properties of individual GMCs in more distant molecule-rich galaxies will rely upon future improvements in angular resolution and sensitivity. At present, some information can be gleaned from single-dish spectra of the regions in multiple tracers of molecular gas. The observations of *Gao and Solomon* (2004) and *Narayanan et al.* (2005) show that the star formation rate is linearly proportional to the mass of molecular gas found at high densities ($\geq 10^5$ cm^{-3}), and that the fraction of dense gas increases with the amount of molecular mass in the system. Since the fraction of molecular mass found at high densities is relatively small in Galactic GMCs, this implies there are substantial differences in GMC properties in these starburst systems.

6. STAR FORMATION IN EXTRAGALACTIC GMCs

The evolution of GMCs substantially influences the evolution of galaxies. In particular, star formation in GMCs is a central event that affects galactic structure, energetics, and chemistry. A detailed understanding of star formation is therefore an important step for a better understanding of galaxy evolution.

6.1. Identification of Star Formation

In Galactic molecular clouds, we are able to study the formation of stars from high mass to low mass including even brown dwarfs. In all external galaxies, even those in the Local Group, such studies are limited to only the highest mass stars as a result of limited sensitivity. It is nonetheless worthwhile to learn how high-mass stars form in GMCs because high-mass stars impart the highest energies to the ISM via UV photons, stellar winds, and supernova explosions.

Young, high-mass stars are apparent at optical/radio wavelengths as the brightest members of stellar clusters or associations or by the Hα and radio continuum emission from H II regions. The positional coincidence between these signposts of star formation and GMCs is the most common method of identifying the star formation associated with individual clouds. Such associations can be made with reasonable confidence when the source density is small enough that confusion is not important. When confusion becomes significant, however, conclusions can only be drawn by either making more careful comparisons at higher angular resolution should or by adopting a statistical approach.
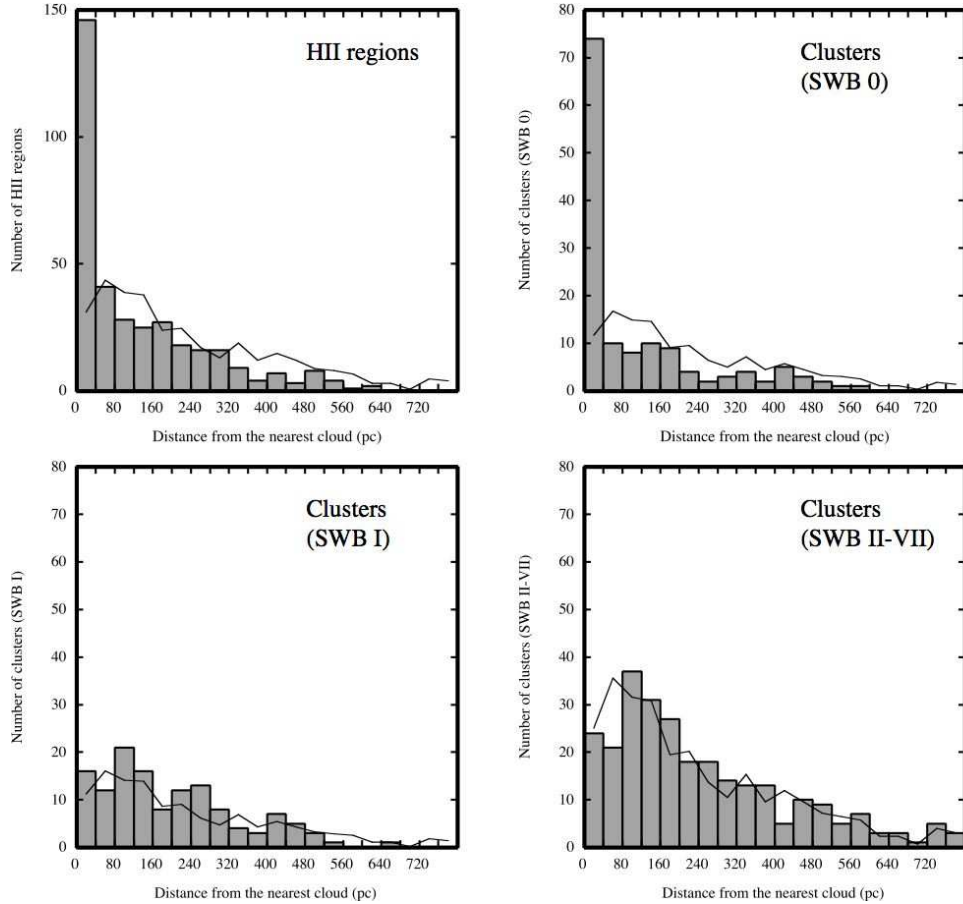
Fig. 11.— Histograms of the projected separation from the H II regions (*Top left Davies et al.* 1976) and clusters cataloged by *Bica et al.* (1996) to the neareset CO emission; (*Top right*) clusters with $\tau < 10$ Myr (SWB 0), (*Bottom left*) clusters with 10 Myr $< \tau < 30$ Myr (SWB I), and (*Bottom right*) clusters with 30 Myr $< \tau$ (SWB II - VII), respectively. The lines represent the frequency distribution expected if the same number of the clusters are distributed at random in the observed area.

6.2. The Large Magellanic Cloud

The most complete datasets for young stars are available for the LMC, which has a distance of 50 kpc. They include catalogs of clusters and associations (e.g., *Bica et al.*, 1996) and of optical and radio H II regions (*Henize*, 1956, *Davies et al.*, 1976, *Kennicutt and Hodge*, 1986, *Filipovic et al.*, 1998). The colors of the stellar clusters are studied in detail at four optical wavelengths and are classified into an age sequence from SWB0 to SWB VII, where SWB0 is the youngest with an age of less than 10 Myr, SWB I in a range 10–30 Myr, and so on (*Bica et al.*, 1996). The sensitivity limit of the published catalogs of star clusters is 14.5 mag (V); it is not straightforward to convert this into the number of stars since a stellar mass function must be assumed. The datasets of H II regions have a detection limit in Hα flux of 10^{-12} ergs cm^{-2} s^{-1}, and the radio sensitivity limit at 5 GHz thermal emission corresponds to 20 mJy. The faintest detectable H II regions correspond to the ionization by an O5 star if a single ionizing source is assumed. We note that the detection limit of H II regions is quite good, $L(\mathrm{H}\alpha) = 2 \times 10^{36}$ ergs s^{-1}, corresponding to one-fourth

the luminosity of the Orion Nebula.

Using the first NANTEN CO survey (*Fukui et al.*, 1999; *Mizuno et al.*, 2001b), the GMCs in the LMC were classified into the three categories according to their associated young objects (*Fukui et al.*, 1999; *Yamaguchi et al.*, 2001c):

I Starless GMCs (no early O stars); "starless" here indicates no associated early O star capable of ionizing an H II regions, which does not exclude the possibility of associated young stars later than B-type

II GMCs with H II regions only; those with small H II regions whose Hα luminosity is less than 10^{37} erg s^{-1}

III GMCs with H II regions and stellar clusters; those with stellar clusters and large H II regions of Hα luminosity greater than 10^{37} erg s^{-1}.

The new NANTEN GMC catalog (*Fukui et al.*, 2006) is used to improve and confirm the statistics of these three classes (*Kawamura et al.*, 2006). For the updated sample of 181 GMCs in Fig. 1, Fig. 11 shows the frequency distribution of the apparent separation of young objects, i.e., optical
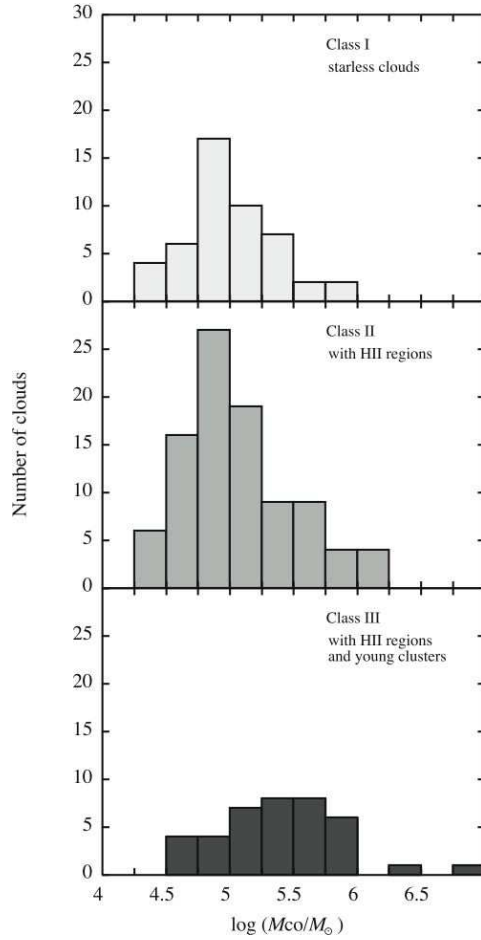
Fig. 12.— Histograms of the mass of class I (*Top*), class II (*Middle*), and class III (*Bottom*), respectively. Mass is derived by using $X_{CO} = 5.4 \times 10^{20}$ cm^{-2}(K km s^{-1})$^{-1}$ (Table 2).
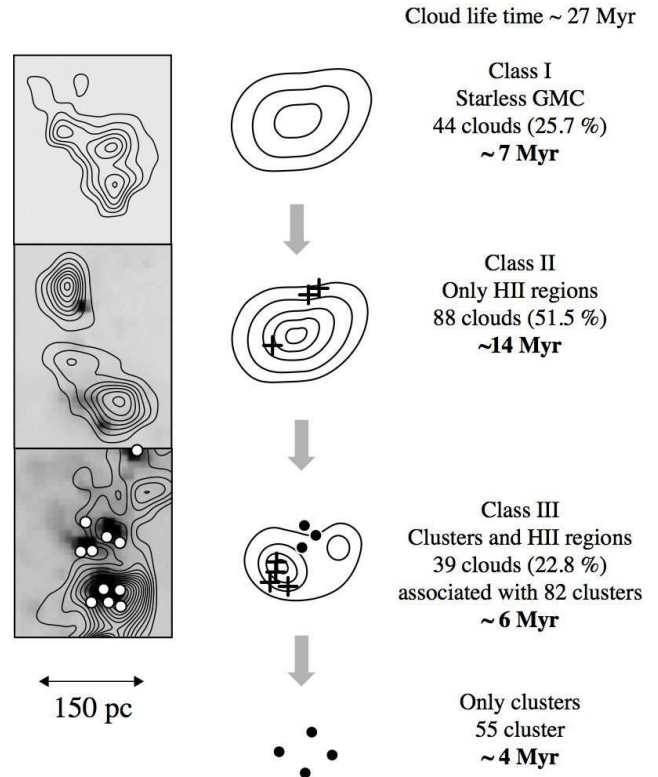

Fig. 13.— Evolutionary sequence of the GMCs in the LMC. An example of the GMCs and illustration at each class are shown in the left panels and the middle column, respectively. The images and contours in the left panels are Hα (*Kim et al.*, 1999) and CO integrated intensity by NANTEN (*Fukui et al.*, 2001; *Fukui et al.*, in preparation); contour levels are from K km s^{-1}with 1.2 K km s^{-1}intervals. Crosses and filled circles indicate the position of the H II regions and young clusters, SWB 0 (*Bica et al.*, 1996), respectively. The number of the objects and the time scale at each class are also presented on the right.

H II regions and stellar clusters, measured from the lowest contour of the nearest GMC. Obviously, the youngest stellar clusters, SWB0 and H II regions, exhibit marked peaks within 50-100 pc, indicating their strong concentrations towards GMCs. Comparisons of these distributions with a purely random distribution is shown by lines. The differences between these peaks are significant. The correlation with young clusters establishes the physical association of the young objects with the GMCs. On the other hand, clusters older than SWB I show almost no correlation with GMCs.

In order to look for any optically obscured H II regions we have also used the Parkes/ATNF radio continuum survey carried out at five frequencies 1.4, 2.45, 4.75, 4.8, and 8.55 GHz (*Filipovic et al.*, 1995, 1998). The typical sensitivity limits of these new datasets are quite good, allowing us to reach flux limits equivalent to those in Hα. The radio continuum results are summarized in a catalog of 483 sources, and the spectral information makes it possible to select H II regions and eliminate background sources not related the LMC. By comparing these data with the GMCs, we found that all of the starless GMCs have no embedded H II re-

gions that are detectable at radio wavelengths (*Kawamura et al.*, 2006).

Table 4 summarizes the results of the present comparison between GMCs and young objects, SWB0 clusters and the H II regions including radio sources. It shows that $\sim 25\%$ of the GMCs are starless in the sense that they are not associated with H II regions or young clusters. Fig. 12 shows mass histograms of the three classes, I, II and III. These indicate that the mass range of the three is from $10^{4.5} M_{\odot}$ to a few times $10^{6} M_{\odot}$. It is also noteworthy that class I GMCs tend to be less massive than the other two in the sense that the number of GMCs more massive than $10^{5} M_{\odot}$ is about half of those of class II and class III GMCs, respectively.

6.3. The Evolution of GMCs in the LMC

The completeness of the present GMC sample covering the whole LMC enables us to infer the evolutionary timescales of the GMCs. We assume a steady state evolution and therefore time spent in each phase is proportional

TABLE 4

ASSOCIATION OF THE YOUNG OBJECTS WITH GMCs

Class of GMC	Number of GMCs[a]	Time scale[b] (Myr)	Association
Class I	44 (25.7 %)	7	Starless
Class II	88 (51.5 %)	14	H II regions
Class III	39 (22.8 %)	6	H II regions and clusters[c]

[a]GMCs with $M > 10^{4.5} M_\odot$; mass is derived by using $X_{CO} = 5.4 \times 10^{20}$ cm^{-2}(K km s^{-1})$^{-1}$ (Table 2).

[b]A steady state evolution is assumed. The absolute time scale is based on the age of stellar clusters; the age of SWB0 clusters, a half of which are associated with the GMCs, is taken to be 10 Myr.

[c]Young clusters or associations, SWB 0, by *Bica et al.* (1996).

to the number of objects in Table 4. Fig. 13 is a scheme representing the evolution suggested from Table 4. The absolute time scale is based on the age of stellar clusters: the age of SWB 0 clusters is taken to be 10 Myr. The first stage corresponds to starless GMCs, having a long time scale of 7 Myr. This is followed by a phase with small H II regions, implying the formation of a few to several O stars. The subsequent phase indicates the most active formation of rich clusters including many early O stars (one of such an example is N 159N). In the final phase, the GMC has been more or less dissipated under the strong ionization and stellar winds from O stars. The lifetime of a typical GMC in the LMC is then estimated as the total of the timescales in Table 4: ~ 27 Myr, assuming that the GMC is completely disrupted by the star formation. As noted earlier (Section 6), the mass of class I GMCs tends to be smaller than the rest. We may speculate that class I GMCs, and possibly part of class II GMCs, are still growing in mass via mass accretion from their surrounding lower density atomic gas. In addition, the lifetime of GMCs likely varies with cloud mass, so 27 Myr is only a characteristic value and is probably uncertain by about 50%.

6.4. Star Formation in M 33

None of the other galaxies in our sample has as complete a record of interstellar gas and star formation as does the LMC, which is due, in part, to its proximity. Nevertheless, it is possible to draw some conclusions about the star formation in M33. *Engargiola et al.* (2003) correlated the H II regions cataloged by *Hodge et al.* (1999) with the 149 GMCs in the M33 catalog. For reference, the completeness limit of the *Hodge et al.* (1999) catalogue is $L(H\alpha) = 3 \times 10^{35}$ erg s^{-1}; a similar range of H II regions is cataloged in the LMC and M33. *Engargiola et al.* (2003) assumed that an H II region is associated with a GMC if its boundary lies either within or tangent to a GMC; 36%

of the flux from H II regions can be associated with the cataloged GMCs. Correcting for the incompleteness of the GMCs cataloged below their sensitivity limit suggests that $> 90\%$ of the total flux of ionized gas from M33 originates from GMCs. Within the uncertainties, essentially all of the flux from H II regions is consistent with an origin in GMCs. Apparently, about half of the star formation in M33 originates in GMCs below the the sensitivity limit of our survey.

A related question is to ask, what fraction of GMCs in M33 is actively forming stars? *Engargiola et al.* (2003) counted the fraction of GMCs with at least one H II region having a separation Δr. They defined the correlation length, such that half the GMCs have at least one H II region within this distance. The correlation length for the GMCs and H II regions is 35 pc; a random distribution of GMCs and H II regions would return a correlation length of 80 pc. They assumed that a GMC is actively forming stars if there is an H II region within 50 pc of the centroid of a GMC. With this assumption, as many as 100 GMCs (67 %) are forming massive stars. Of the 75 GMCs with masses above the median cataloged mass, the fraction of clouds actively forming stars rises to 85%. They estimate that the number of totally obscured H II regions affect these results by at most 5%.

Thus the fraction of GMCs without star formation is estimated to be about 1/3, a fraction similar to that in the LMC. The M33 study estimated the lifetime of GMCs to be ~ 20 Myr, also similar to that found for the LMC. The fraction of clouds without active star formation is much higher than that found in the vicinity of the Sun where only one of all of the GMCs within 2 kpc is found to be devoid of star formation. It is unclear whether this difference is significant. Neither the LMC analysis, nor the M33 analysis would detect the low-mass star formation which it is proceeding in the Taurus molecular clouds. In any event, both the LMC and M33 studies suggest that the fraction of clouds without star formation is small. Thus the onset of star formation in GMCs is rather rapid not only in the Milky Way, but in at

least some lower mass spiral and irregular galaxies.

7. FUTURE PROSPECTS

Studying GMCs in galaxies using CO emission requires spatial resolutions higher than 30–40 pc. It will be possible to extend studies such as ours to a few tens of Mpc soon, with the advent of ALMA and CARMA arrays in the southern and northern hemispheres respectively. These instruments will provide angular resolutions of 0.1–1 arcsec in millimeter and sub-millimeter CO emission, corresponding 5–50 pc at 10 Mpc and will provide unprecedented details of physical conditions in GMCs in galaxies. The work described in this chapter should be just the beginning of extragalactic GMC studies.

8. SUMMARY AND CONCLUSIONS

We have compared the properties of GMCs in 5 galaxies, four of which have been surveyed in their entirety: the LMC, the SMC, M33, IC 10. M31 was observed over a very limited area. The interstellar medium of all five galaxies is dominated by the atomic phase.

1. The GMCs do not, in general, show any relationship to the stellar content of the galaxies except for the O stars born in the GMCs.

2. There is a very good correlation between the locations of the GMCs and filaments of H I. Many filaments contain little of no molecular gas even though they have similar surface densities compared to those that are rich in GMCs. This suggests that clouds form from the H I rather than vice-versa.

3. There appears to be a clear evolutionary trend going from filament formation → molecule formation → GMC formation. It is not clear however, whether the condensations that form GMCs are first formed in the atomic filaments, or only after the molecules have formed.

4. We derive X_{CO} for all of the galaxies assuming that the GMCs are virialized. Although there is some variation, a value of $X_{CO} = 4 \times 10^{20}$ cm^{-2} (K km s^{-1})$^{-1}$ is a representative value to within about 50% except for the SMC, which has a value more than 3 times higher. There is no clear trend of X_{CO} with metallicity.

5. The discrepancy between the virial value and the value determined from γ-ray observations in the Milky Way suggests that the GMCs are not virialized, if the γ-ray value is applicable to other galaxies in the Local Group. In that case, a value of $X_{CO} = 2 \times 10^{20}$ cm^{-2} (K km s^{-1})$^{-1}$ may be more appropriate.

6. The GMCs in our sample appear to satisfy the line width-size relation for the Milky Way, but with an offset in the constant of proportionality. This offset may be due, at least in part, to the different data analysis techniques for the MW and extragalactic data sets. For a given line width, the extragalactic clouds appear to be about 50 % larger. Despite the systematic offset, there are small but significant differences in the line width-size relationship among GMCs in different galaxies.

7. The GMCs within a particular galaxy have a roughly constant surface density. If the value of X_{CO} we derive for each galaxy is applied, the surface densities of the sample as a whole, have a scatter of less than a factor of two.

8. The mass spectra for the GMCs in all of the galaxies can be characterized as a power law with a slope of ~ -1.7, with the exception of M33, which has a slope of -2.5.

9. The ratio of H$_2$ to H I on a pixel-by-pixel basis in galaxies appears to be determined by the hydrostatic pressure in the disk.

10. About 1/4 – 1/3 of the GMCs in the LMC and M33 appear to be devoid of high-mass star formation.

11. The association of stars and H II regions in the LMC suggests a lifetime for the GMCs of about 27 Myr, with a quiescent phase that is about 25% of the age of the GMCs. In M33, a lifetime of ~ 20 Myr is measured. For GMCs in these galaxies we estimate that typical lifetimes are roughly 20–30 Myr. Both lifetimes are uncertain by about 50%.

REFERENCES

Allen R. J. (2001) In *ASP Conf. Ser. 240: Gas and Galaxy Evolution 240*, (J. Hibbard and J. van Gorkom, eds.), pp. 331-337. ASP Conf. Series, San Francisco.

Bica E., Claria J. J., Dottori H., Santos J. F. C. Jr., and Piatti A. E., (1996) *Astrophys. J. Suppl.*, *102*, 57-73.

Blitz L. and Rosolowsky E. (2004), *Astrophys. J.*, *612*, L29-L32.

Blitz L. and Rosolowsky E. (2006), submitted.

Bolatto A. et al. (2006), in preparation.

Braun R., Walterbos R. A. M., Kennicutt R. C., and Tacconi L. J. 1994, *Astrophys. J.*, *420*, 558-569.

Cohen R. S., Dame T. M., Garay G., Montani J., Rubio M., and Thaddeus P. 1988, *Astrophys. J.*, *331*, L95-L99.

Dame T., M., Hartmann D., and Thaddeus P. (2001) *Astrophys. J.547*, 792-813.

Davies R. D., Elliott K. H., and Meaburn J. (1976) *Mem. R. Astron. Soc.*, *81*, 89-128.

de Boer K. S., Braun J. M., Vallenari A., and Mebold U. (1998), *Astron. Astrophys.*, *329*, L49-L52.

Deul E. R. and van der Hulst J. M. (1987) *Astron. Astrophys. Suppl.67*, 509-539.

Elmegreen B. G. (1993), *Astrophys. J.*, *411*, 170-177.

Engargiola G., Plambeck R. L, Rosolowsky E., and Blitz L. (2003) *Astrophys. J. Suppl.*, *149*, 343-363.

Filipovic M. D., Haynes R. F., White G. L., Jones P. A., Klein U., and Wielebinski R. (1995), *Astron. Astrophys. Suppl.*, *111*, 311-332.

Filipovic M. D., Haynes R. F., White G. L., and Jones P. A. (1998), *Astron. Astrophys. Suppl.*, *130*, 421-440.

Fujimoto M. and Noguchi M. (1990) *Publ. Astron. Soc. Japan, 42*, 505-516.

Fukui Y., Mizuno N., Yamaguchi R., Mizuno A., Onishi T., et al. (1999) *Publ. Astron. Soc. Japan, 51*, 745-749.

Fukui Y., Mizuno N., Yamaguchi R., Mizuno A., and Onishi T. (2001) *Publ. Astron. Soc. Japan Letters, 53*, L41-L44.

Fukui Y. et al. (2006), in preparation.

Gao Y. and Solomon P. M. (2004), *Astrophys. J.*, *606*, 271-290.

Gerola H. and Seiden P. E. (1978) *Astrophys. J.*, *223* 129-135.

Helfer T. T. and Blitz L. (1993), *Astrophys. J.*, *419*, 86-93.

Helfer T. T., Thornley M. D., Regan M. W., Wong T., Sheth K., Vogel S. N., Blitz L., and Bock D. C.-J. (2003), *Astrophys. J. Suppl.*, *145*, 259-327.

Henize K. G. (1956), *Astrophys. J. Suppl.*, *2*, 315-344.

Henry R. B. C. and Howard J. W. (1995), *Astrophys. J.*, *438*, 170-180.

Heyer M. H., Carpenter J. M., and Snell R. L. (2001), *Astrophys. J.*, *551*, 852-866.

Hodge P. W., Balsley J., Wyder T. K., and Skelton B. P. (1999), *Publ. Astron. Soc. Pac.*, *111*, 685-690.

Jarrett T. H., Chester T., Cutri R., Schneider S. E., and Huchra J. P. (2003), *Astron. J.*, *125*, 525-554.

Kawamura A. et al. (2006) in preparation.

Kennicutt R. C. (1998), *Astrophys. J.*, *498*, 541-552.

Kennicutt R. C. Jr. and Hodge P. W. (1986) *Astrophys. J.*, *306*, 130-141.

Keto E., Ho L., and Lo K.Y. (2005), astro-ph/0508519.

Kim S., Staveley-Smith L., Dopita M. A., Freeman K. C., Sault R. J., Kesteven M. J., and McConnell D. (1998), *Astrophys. J.*, *503*, 674-688.

Kim S., Staveley-Smith L., Dopita M. A., Sault R. J., Freeman K. C., Lee Y., and Chu Y.-H. (2003), *Astrophys. J. Suppl.*, *148*, 473-486.

Kregel M., van der Kruit P. C., and de Grijs R. 2002, *Mon. Not. R. Astron. Soc.*, *334*, 646-668.

Koornneef J. (1984) In *IAU Symp. 108, Structure and Evolution of the Magellanic Clouds*, (S. van den Bergh and K. S. de Boer,

eds.), pop. 333-339, D. Reidel, Dordrecht.

Lada C. J., Margulis M., Sofue Y., Nakai N., and Handa T. (1988), *Astrophys. J.*, *328*, 143-160.

Leroy A., Bolatto, A., Walter, F., and Blitz, L. (2006), *Astrophys. J.*, in press.

Massey P., Hodge P. W., Holmes S., Jacoby G., King N. L., Olsen K., Saha A., and Smith C. (2001), *Bull. Am. Astron. Soc.*, *33*, 1496.

Mizuno N., Rubio M., Mizuno A., Yamaguchi R., Onishi T., and Fukui Y. (2001a), *Pub. of Astron. Soc. Japan, 53*, L45-L49.

Mizuno N., Yamaguchi R., Mizuno A., Rubio M., Abe R., Saito H., Onishi T., Yonekura Y., Yamaguchi N., Ogawa H., and Fukui Y. (2001b), *Pub. of Astron. Soc. Japan, 53*, 971-984.

Mizuno N. et al. (2006) in preparation.

Narayanan D., Groppi C. E., Kulesa C. A., and Walker C. K. (2005), *Astrophys. J.*, *630*, 269-279.

Oka T., Hasegawa T., Sato F., Tsuboi M., Miyazaki A., and Sugimoto M. (2001), *Astrophys. J.*, *562*, 348-362.

Regan M. and Vogel S. (1994) *Astrophys. J.*, *434*, 536-545.

Rosolowsky E. (2006), *Astrophys. J.*, submitted.

Rosolowsky E. and Leroy A. (2006), *Publ. Astron. Soc. Pac.*, in press.

Rosolowsky E. and Blitz L. (2005) *Astrophys. J.623* 826-845.

Rosolowsky E., Plambeck R., Engargiola G., and Blitz L. (2003) *Astrophys. J.599* 258-274.

Rubio M., Garay G., Montani J., and Thaddeus P. (1991), *Astrophys. J.*, *368*, 173-177.

Solomon P. M., Rivolo A. R., Barrett J. and Yahil A. (1987) *Astrophys. J.319*, 730-741.

Spergel D. N. and Blitz L. (1992), *Nature*, *357*, 665-667.

Stanimirović S., Staveley-Smith L., Dickey J. M., Sault R. J., and Snowden S. L. (1999), *Mon. Not. R. Astron. Soc.*, *302*, 417-436.

Stanimirović S., Staveley-Smith L., van der Hulst J. M., Bontekoe T. R., Kester D. J. M., and Jones P. A. (2000), *Mon. Not. R. Astron. Soc.*, *315*, 791-807.

Strong A. W. and Mattox J. R. (1996) *Astron. Astrophys.*, *308*, L21-L24.

van der Kruit P. C. and Searle L. (1981a), *Astron. Astrophys.*, *95*, 105-115.

van der Kruit P. C. and Searle L. (1981b), *Astron. Astrophys.*, *95*, 116-126.

Vogel S. N., Boulanger F., and Ball R. (1987), *Astrophys. J.*, *321*, L145-L149.

Wilcots E. M. and Miller B. W. (1998) *Astron. J.116*, 2363-2394.

Williams J. P. and McKee C. F. (1997), *Astrophys. J.*, *476*, 166-183.

Wilson C. D. (1994), *Astrophys. J.*, *434*, L11-L14.

Wilson C. D. and Reid I. N. (1991), *Astrophys. J.*, *366*, L11-L14.

Wilson C. D. and Rudolph A. L. (1993), *Astrophys. J.*, *406*, 477-481.

Wilson C. D. and Scoville N. (1990) *Astrophys. J.*, *363*, 435-450.

Wong T. and Blitz L. (2002), *Astrophys. J.*, *569*, 157-183.

Yamaguchi R., Mizuno N., Onishi T., Mizuno A., and Fukui Y. (2001a), *Astrophys. J.*, *553*, L185-L188.

Yamaguchi R., Mizuno N., Onishi T., Mizuno A., and Fukui Y. (2001b), *Pub. of Astron. Soc. Japan, 53*, 959-969.

Yamaguchi R., Mizuno N., Mizuno A., Rubio M., Abe R.,Saito H., Moriguchi Y., Matsunaga L., Onishi T., Yonekura Y., and Fukui Y. (2001c), *Pub. of Astron. Soc. Japan, 53*, 985-1001.